

❸ One-Month-Lead Predictability of Asian Summer Monsoon Indices Based on the Zonal Winds by the APCC Multimodel Ensemble❹

HYE-JIN PARK

Division of Earth Environmental System, Pusan National University, Busan, South Korea

VLADIMIR N. KRYJOV

Hydrometeorological Research Center, Moscow, Russia

JOONG-BAE AHN

Division of Earth Environmental System, Pusan National University, Busan, South Korea

(Manuscript received 5 December 2017, in final form 6 August 2018)

ABSTRACT

The seasonal predictability of Asian summer monsoon indices characterizing horizontal and vertical zonal wind shear is investigated using 1-month-lead hindcast datasets from seven coupled global circulation models (CGCMs) participating in the operational multimodel ensemble (MME) seasonal prediction system of the Asia-Pacific Economic Cooperation Climate Center (APCC) for the 1983–2010 period. The summer monsoon indices analyzed in this study represent the South Asian summer monsoon (SASM), western North Pacific summer monsoon (WNPSM), and the newly defined northeastern Asian summer monsoon (NEASM). For the WNPSM and NEASM indices, we also analyze the prediction skill of the index components separately. The study demonstrates that the operational APCC MME system reliably predicts most of the summer monsoon indices and their components, with correlation coefficients exceeding the 99% confidence level. Analysis of the ocean sources of the prediction skill of the indices reveals that the strong relationships of most of the monsoon indices and their components with sea surface temperature (SST) are not confined to the equatorial Pacific but rather are dispersed throughout the World Ocean, with the leading role played by the north Indian Ocean SST anomalies. This conclusion is supported by the analysis of correlations between the monsoon indices and the tropical SST indices. The correlations between the SST anomalies and all the summer monsoon indices in the MME predictions are stronger than those in the observations. However, overestimation of the role of the ENSO-related SST anomalies in the seasonal model hindcasts results in some predictability deterioration of the SASM and NEASM indices.

1. Introduction

Asian summer monsoons affect the most populated region of the world, with floods and droughts caused by monsoon anomalies impacting both the regional economies and societies. Seasonal prediction of the Asian

summer monsoon rainfalls is one of the crucial tasks of the prediction community. However, direct dynamical seasonal predictions of the Asian monsoon rainfall anomalies are not yet reliable (Kang et al. 2002; Sohn et al. 2012; Yuan et al. 2015; Min et al. 2017), mainly because of the complexity of the precipitation formation and its inadequate simulation by dynamical models (e.g., Wang et al. 2009). Meanwhile, rainfall anomalies in the region are closely related to circulation anomalies (e.g., Wang et al. 2008), which affect both moisture delivery to the region (Ding 2004; Ding and Chan 2005; Day et al. 2015) and dynamical conditions of its convection (Wang et al. 2008). Dynamical model predictions of the circulation anomalies over the region are more reliable than those of precipitation (Wang et al. 2009;

❸ Denotes content that is immediately available upon publication as open access.

❹ Supplemental information related to this paper is available at the Journals Online website: <https://doi.org/10.1175/JCLI-D-17-0816.s1>.

Corresponding author: Prof. Joong-Bae Ahn, jbahn@pusan.ac.kr

Lee and Wang 2012; D. Y. Lee et al. 2013). The monsoon rainfall anomalies are strongly related to certain circulation patterns, which can be presented by monsoon circulation indices. Particularly, Webster and Yang (1992) have suggested an index describing the broad-scale South Asian summer monsoon [SASM; Webster–Yang index (WYI)], defined as a difference between the lower- and upper-troposphere zonal wind anomalies over the northern tropical Indian Ocean. Goswami et al. (1999) have suggested an index characterizing a broad Hadley cell over the Indian subcontinent [monsoon Hadley circulation index (MHI)] based on the difference in the meridional wind anomalies in the lower and upper troposphere. A set of indices has been developed by Wang and Fan (1999) covering both South Asian and western North Pacific summer monsoons (WNPSMs) based both on vertical wind shear between the lower and upper troposphere and on the horizontal shear (vortex) in the lower troposphere. Because of their clear physical meaning, strong relationships with the regional rainfalls, and simple definition, these indices are widely used by meteorological services of the countries of South and East Asia. A number of the Asian summer monsoon indices have also been suggested in other studies (e.g., Shi and Zhu 1996; Lau et al. 2000; Li and Zeng 2002; Ha et al. 2005).

The predictability of the Asian summer monsoon indices by the dynamical models has been analyzed in recent years. Several studies (Yang et al. 2008; Zhou et al. 2009b; Kim et al. 2012; Lu et al. 2012; Li et al. 2014; Jung et al. 2015) have shown a good predictability by operational models National Centers for Environmental Prediction (NCEP) CFS, NCEP CFSv2, ECMWF System 4, the Met Office Global Seasonal Forecast System, version 5 (GloSea5), and the models participating in the ENSEMBLES project of the western North Pacific monsoon index (WNPMI) defined by Wang and Fan (1999) and slightly modified by B. Wang et al. (2001). A similar high level of predictability is featured by WYI (Yang et al. 2008; Zhou et al. 2009a; Kim et al. 2012). MHI was well predicted by CFS (Yang et al. 2008) with a correlation of about 0.6. However, less predictable (correlations less than 0.3) are the Indian monsoon index of B. Wang et al. (2001) based on the low-troposphere vortex over India (Zhou et al. 2009a; Kim et al. 2012), the extratropical western North Pacific circulation indices (Yang et al. 2008; Jung et al. 2015) suggested by Lau et al. (2000), the upper-troposphere vortex, and the low-troposphere wind index suggested by Ha et al. (2005). Summarizing the published results from the studies on the predictability of the Asian monsoon indices suggests that most of the state-of-the-art coupled global circulation models (CGCMs) are able

to skillfully predict seasonal-mean large-scale SASM indices, WYI and MHI, and tropical–subtropical WNPMI. However, the predictability of the western SASM circulation indices and extratropical East Asian summer monsoon (EASM) indices remains low compared to other SASM indices (e.g., Yang et al. 2008; Zhou et al. 2009a).

In this paper we analyze the prediction skill of the SASM and EASM monsoon indices obtained from a set of operational models comprising the Asia–Pacific Economic Cooperation Climate Center (APCC) operational model suit. The study is based on the 1-month-lead historical predictions by seven operational CGCMs. Since the study assesses the prediction skill of the monsoon indices for use in operational predictions, we focus on several widely used indices covering both SASM and EASM that will be described in section 2. For the indices combined with tropical and subtropical components, along with the index itself, we analyze the prediction skill of each component separately. Since well-predictable WNPMI characterizes precipitation mainly in the tropical western North Pacific and the southern part of East Asia, we have defined a new circulation monsoon index for the northern part that is strongly correlated with precipitation in the middle latitudes of East Asia. Although the Asian monsoons and Australian monsoons constitute the unified Asian–Australian monsoon system, we do not assess the prediction skill of the Australian monsoon indices because we focus on the boreal summer Asian rainy season.

Section 2 briefly describes the observations, hindcast datasets, and summer monsoon indices used in this study. Section 3 examines the prediction skill of the summer monsoon indices. In section 4 we analyze and discuss the sources of predictability of the monsoon indices. Section 5 summarizes the study findings.

2. Data and methodology

The boreal summer [June–August (JJA)] hindcast outputs from seven CGCMs participating in the operational multimodel ensemble (MME) seasonal prediction system of APCC are used in this study. These hindcasts have the common period of 1983–2010 (28 years). Model integrations were initialized in May of each year, that is, with a 1-month lead. A brief description of the models is presented in Table 1. All hindcast data are interpolated to a 2.5° latitude \times 2.5° longitude grid across the globe. A simple averaged MME is applied using the seven CGCMs (Min et al. 2014). It should be noted that the 28-yr length of the hindcast series strongly restricts the statistical significance of the obtained results and there is a need for prolonged hindcasts that are up to date.

TABLE 1. Description of the models used in this study.

Institute (Country)	Model name	AGCM (Resolution)	OGCM (Resolution)	Ensemble size	Period of hindcast
APCC (South Korea)	CCSM3	CAM3.0 (T85L26)	POP1.3 (gx1v3 L40)	10	1983–2014
BoM (Australia)	POAMA	BAM (T47L17)	ACOM2 (0.5°–1.5° lat × 2.0° lon L25)	33	1983–2011
MSC_CanCM3 (Canada)	CGCM3	CGCM3 (T63L31)	OGCM4 (1.41° lon × 0.94° lat L40)	10	1981–2010
MSC_CanCM4 (Canada)	CGCM4	CGCM4 (T63L31)	OCGM4 (1.41° lon × 0.94° lat L40)	10	1981–2010
NASA (United States)	GMAO	GEOS-5 (288 × 181L72)	MOM4 (720 × 410 L40)	11	1982–2012
NCEP (United States)	CFSv2	GFS (T126L64)	MOM4 (0.25°–0.5° lat × 1° lon L40)	20	1982–2010
PNU (South Korea)	PNU CGCM	CCM3 (T42L18)	MOM3 (2.8125° lon × 0.7°–2.8° lat L29)	5	1981–2014

For hindcast evaluation, the wind data at 850 and 200 hPa from the NCEP–DOE AMIP Reanalysis-II (NCEP-2; Kanamitsu et al. 2002) on a 2.5° latitude × 2.5° longitude grid are used. The observed precipitation data are used from Global Precipitation Climatology Project (GPCP), version 2.2 (Adler et al. 2003), with 2.5° latitude × 2.5° longitude spatial resolution. The sea surface temperature (SST) data of National Oceanic and Atmospheric Administration (NOAA) optimum interpolation (OI) SST, version 2 (Reynolds et al. 2002), meshed on a 1° latitude × 1° longitude grid, are interpolated to a 2.5° latitude × 2.5° longitude grid.

Predictions of the monsoon indices based on the zonal wind are assessed because the patterns of zonal wind anomalies basically well represent the variability of the Asian summer monsoon characteristics such as precipitation, convective activity, and vorticity (e.g., Wang et al. 2008). Table 2 and Fig. 1 show the definitions and the domains of the Asian summer monsoon indices used. The SASM indices used in this study are the WYI suggested by Webster and Yang (1992), the westerly shear index1 (WSI1) by Wang and Fan (1999), and the Indian monsoon index (IMI) by B. Wang et al. (2001). WYI and WSI1 represent interannual variability of the broad-scale South Asian summer monsoon, and IMI reflects that of the Indian summer. The westerly shear

index2 (WSI2) by Wang and Fan (1999) and WNPMI (B. Wang et al. 2001) are used as the WNPSM indices, and the newly suggested extratropical northeastern Asian summer monsoon index (NEASMI) is used as the EASM index. WYI, WSI1, and WSI2 are defined based on the vertical wind shear between the lower and upper troposphere. IMI, WNPMI, and NEASMI are defined based on the zonal wind shear representing the vorticity in the lower troposphere. Since model predictabilities in the tropics are higher than in the extratropics (e.g., Li et al. 2012), predictabilities of the southern and northern components of IMI, WNPMI, and NEASMI, named IM_SI, WNPM_SI, NEASM_SI, and IM_NI, WNPM_NI, NEASM_NI, respectively, are assessed separately to evaluate the contribution from each component.

The rank histograms (Hamill 2001) for the ensemble predictions of precipitation and zonal wind at 850 hPa (U850) from the seven models for the tropics (30°S–30°N, 0°–360°E; figures not shown) illustrate very flat distribution for the U850 predictions, suggesting that the zonal-wind-based monsoon indices can be appropriately used as indices in investigating the seasonal prediction skill of SASM and WNPSM.

Among the analyzed indices, NEASMI has been newly defined based on the correlations between summer precipitation over northeastern Asia (30°–50°N,

TABLE 2. Definitions of the summer monsoon indices used in this study. U850 and U200 denote the zonal wind at 850 and 200 hPa, respectively.

Index	Definition	Source
WYI	Zonal wind shear (U850–U200) averaged over 0°–20°N, 40°–110°E	Webster and Yang (1992)
WSI1	Westerly shears (U850–U200) averaged over 5°–20°N, 40°–80°E	Wang and Fan (1999)
IMI	U850 (5°–15°N, 40°–80°E) (IM_SI) minus U850 (20°–30°N, 70°–90°E) (IM_NI)	B. Wang et al. (2001)
WSI2	Westerly shear (U850–U200) averaged over 0°–10°N, 90°–130°E	Wang and Fan (1999)
WNPMI	U850 (5°–15°N, 100°–130°E) (WNPM_SI) minus U850 (20°–30°N, 110°–140°E) (WNPM_NI)	B. Wang et al. (2001)
NEASMI	U850 (25°–35°N, 110°–150°E) (NEASM_SI) minus U850 (45°–55°N, 110°–150°E) (NEASM_NI)	Newly defined

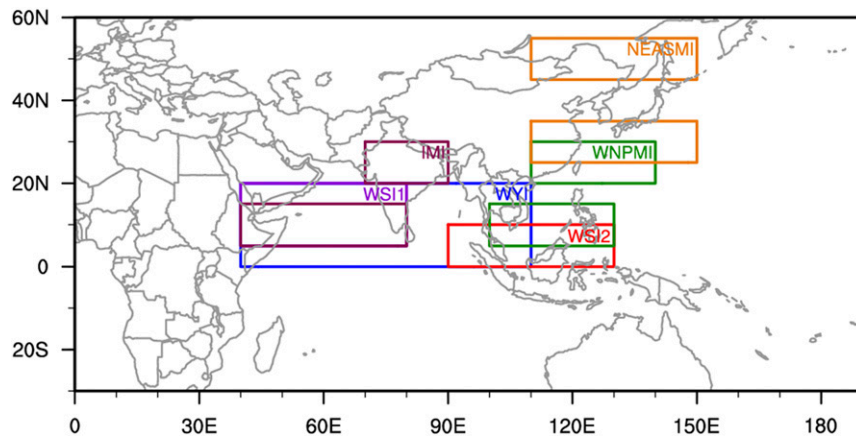


FIG. 1. Domains of the summer monsoon indices used in this study. These indices are defined in the text.

110°–145°E; Lee et al. 2005) and the zonal wind at 850 hPa. Summer precipitation is significantly positively correlated with zonal wind over southern China through southern Japan, and negatively correlated with zonal wind over midlatitude Asia from the Baikal Lake through the Okhotsk Sea and over the Philippine Sea (Fig. 2). We have defined NEASMI as the meridional difference between the zonal winds at 850 hPa averaged over the domains 25°–35°N, 110°–150°E and 45°–55°N, 110°–150°E. Thus, this index presents the lower-troposphere vorticity over the extratropical East Asia region, and its relationships with regional precipitation are physically plausible.

To confirm the precipitation patterns represented by the summer monsoon indices, the correlations between the monsoon indices and summer precipitation were calculated from the observations (Fig. 3). All of the SASM indices positively correlate with precipitation over the Indian subcontinent (Figs. 3a,b,d). However, the regions of significant correlations are different. WYI and WSI1 are positively correlated with precipitation over the northeastern part of the Indian subcontinent, with the area of significant correlations of WYI being narrower than that of WSI1. Also, WYI and WSI1 negatively correlate with precipitation over the Arabian Sea. The region of significant correlations of IMI is the widest among the SASM indices, with the area of the significant positive correlations spanning most of the northern Indian subcontinent. Also, IM_SI significantly correlates with precipitation over the northeastern part of the Indian subcontinent similarly to WYI and WSI1, while IM_NI significantly negatively correlates with precipitation over most of the Indian subcontinent except for the very northeastern part. The SASM indices are significantly correlated with precipitation in remote regions. WYI and WSI1 are positively correlated with precipitation over the northwestern part

of East Asia, and IMI is negatively correlated with precipitation over the northeastern part of East Asia.

The correlation patterns between WSI2 and summer precipitation are similar to those of WNPMI and WNPM_SI. The negative correlation pattern stretches zonally from the Middle East through the Maritime Continent, and the positive pattern spans the region from the Indochina Peninsula through the central Pacific. Also, WSI2, WNPMI, and WNPM_SI have negative correlations with precipitation over central China remotely. The correlation pattern between WNPM_NI and summer precipitation over the western Pacific and East Asia is similar with NEASMI and NEASMI_SI. These indices show the negative correlation patterns over the Philippine Sea and the Sea of Okhotsk and the positive correlation patterns over eastern China through Japan. These patterns closely resemble the Pacific–Japan teleconnection pattern (Kosaka and Nakamura 2006; Kubota et al. 2016). The correlation patterns

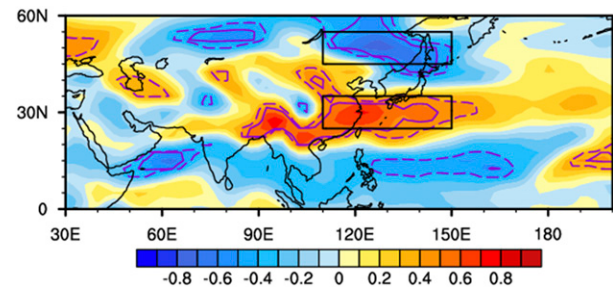


FIG. 2. Correlation map between the zonal wind at the 850-hPa surface (U_{850}) and summer precipitation over northeastern Asia from the observations during 1983–2010. The solid (dashed) contours denote the correlation coefficients significant at the 99% (95%) confidence level. The black-lined boxes indicate the domain of the northeastern Asian summer monsoon index defined in this study.

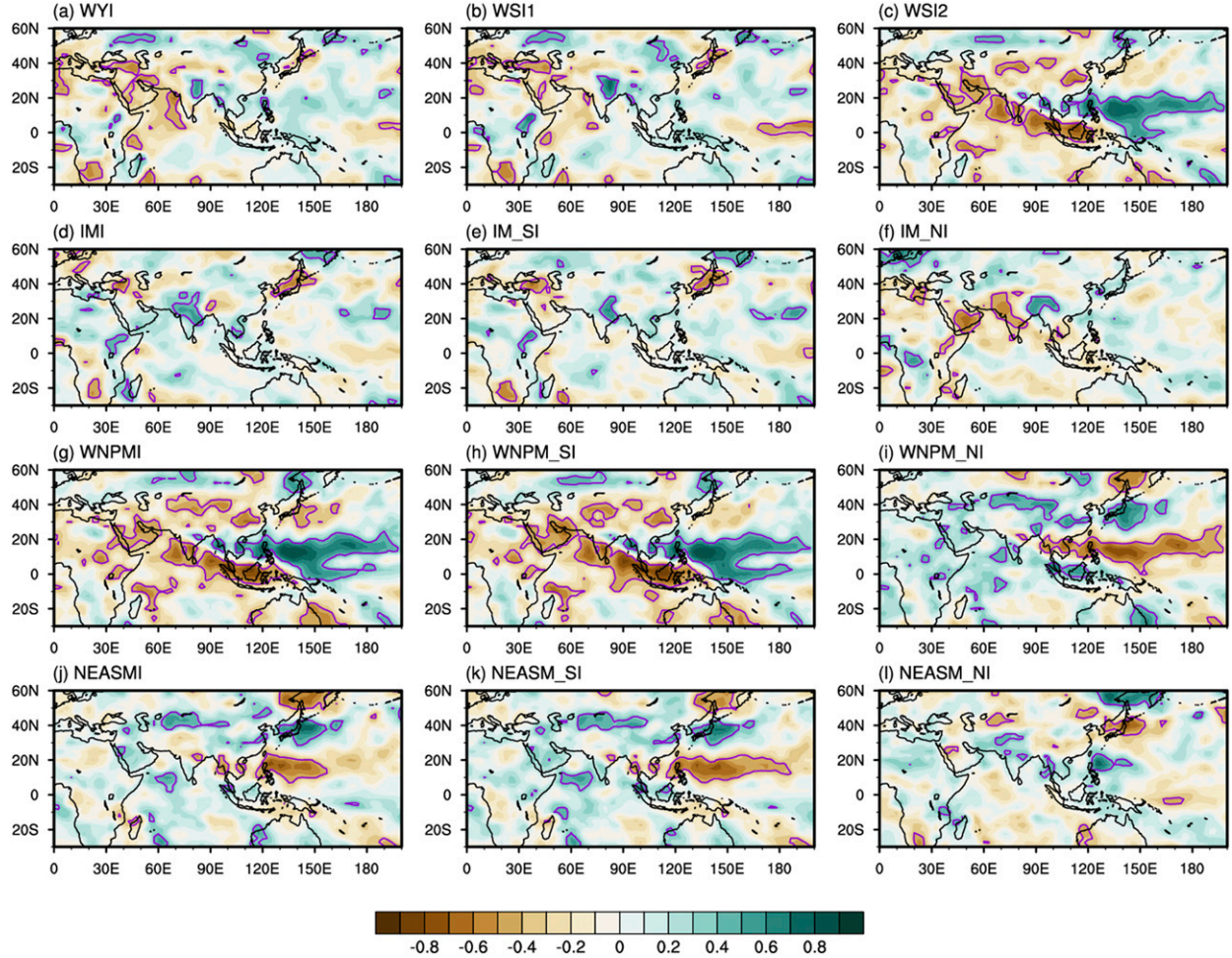


FIG. 3. Correlation maps between summer precipitation and the monsoon indices from the observations during 1983–2010. The contours denote the correlation coefficients significant at the 95% confidence level.

between NEASM_NI and precipitation are the same as for NEASMI, but with the opposite sign.

The seasonal prediction skills of the summer monsoon indices are assessed in terms of the temporal correlation coefficients (TCC). The statistical significance of the TCCs is evaluated using the two-tailed Student's *t* test. The significance of the difference between the TCCs is assessed as the significance of the difference between the Fisher *z*-transformed TCCs (Yule and Kendall 1950; Wilks 1995). The series of observed and predicted indices are serially correlated, so in the significance tests we use the effective sample size estimated following Bretherton et al. (1999).

3. Results

Figure 4 shows the time series of the normalized summer monsoon indices. The black and red solid lines denote the summer monsoon indices of the observations

and MME, respectively, and the dashed lines indicate the indices of individual models. Most of the summer monsoon indices predicted by the MME well follow the interannual variations of the indices derived from the observations, except for IMI and its components and NEASM_NI. Especially, the MME-predicted WNPMI has the highest correlation coefficient with the observations among all the summer monsoon indices. Individual models also basically well represent the interannual variations of the summer monsoon indices derived from the observations.

Table 3 presents the TCCs between the summer monsoon indices obtained from the observations and those from the MME and each model. For SASM, the TCCs of WYI and WSI1 simulated by the MME are 0.54 and 0.63, respectively, which exceed the 99% confidence level (Table 3). TCCs for these indices from most of the individual models exceed the 95% confidence level. WSI1 of all models has a higher TCC than WYI does.

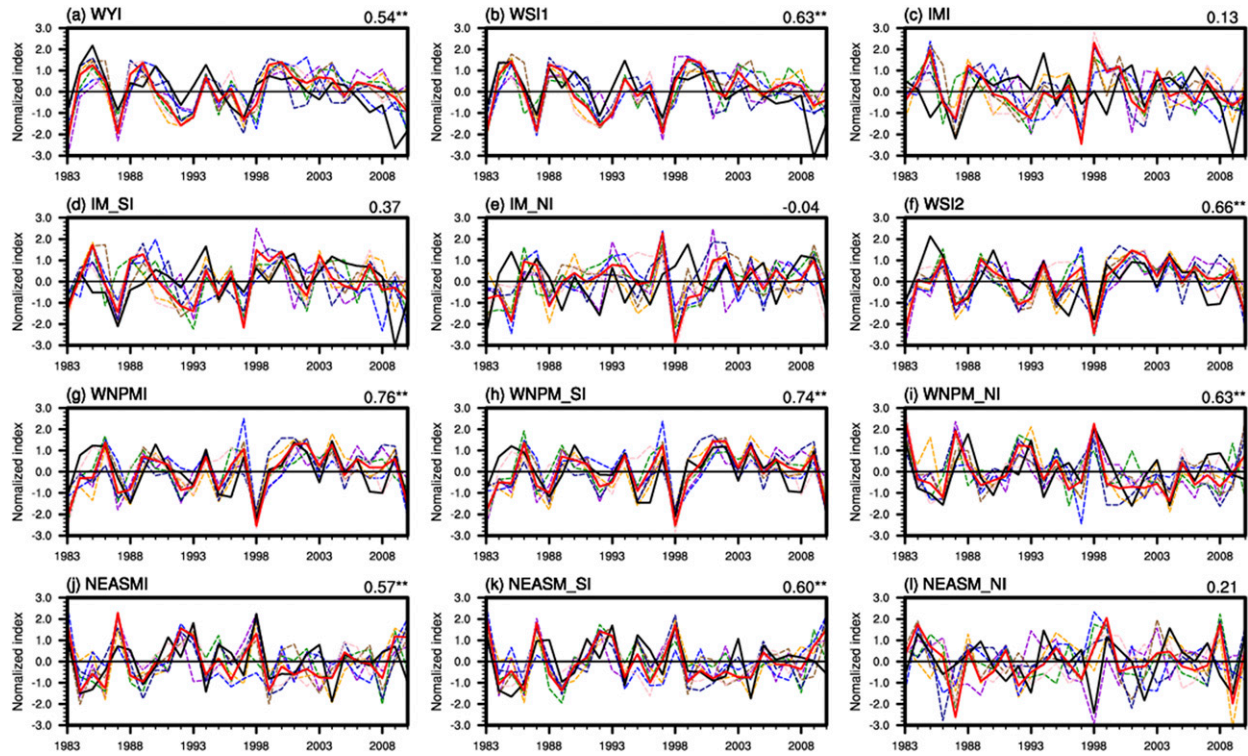


FIG. 4. Time series of the summer monsoon indices derived from the observations (black thick lines), MME (red thick lines), and individual models (dashed lines) during 1983–2010. The number in the upper-right corner of each panel denotes the correlation coefficient between the observed and MME-predicted monsoon indices. The single and double asterisks denote the correlation coefficients statistically significant at the 95% and 99% confidence levels, respectively.

This indicates that the vertical shear of zonal wind from the models is better simulated over the Arabian Sea (WSI1) than over the north Indian Ocean (WYI), although the domain of WYI includes the entire domain of WSI. Unlike the prediction skills of WYI and WSI1, IMI and its components, IM_SI and IM_NI, predicted by the MME and individual models are insignificantly correlated with those from observations. This result corresponds to the results of Zhou et al. (2009a) and Kim et al. (2012), who documented the low prediction skill of IMI. The prediction skills of the components of IMI are different. While correlation between the observed and MME-predicted IM_SI achieves the 90% confidence level, the TCC for IM_NI is close to zero. In Fig. 5a, a large part of the northern domain (IM_NI) features negative correlations between observed and MME-predicted U850.

A possible explanation for this very poor skill of IM_NI is the very complex relief of the domain. The height of the 850-hPa surface is about 1.5 km. Meanwhile the central part of the domain, the Indo-Gangetic Plain, is bordered by Himalayan peaks on the north that are several times higher than 1.5 km, with the large northeastern part of the 1.5-km-height surface being “inside”

the Himalayas where both reanalysis and model winds are mere calculations that do not exist in nature. From the northwest, the domain is bordered by the Hindu Kush and Sulaiman Mountains 2–3-km high, and hills of up to 1-km height are located in the southern part of the domain. Such complex relief implies a variety of local lower-troposphere wind peculiarities that are not simulated by the seasonal prediction models that are skillful in predicting the global- and large regional-scale circulation patterns.

Another question concerns the IM_SI skill. The domain of the IM_SI is very close to that of WSI1 but the skill of WSI1 predictions is much higher, with a correlation of 0.63 for predictions with MME, which is significant at the 99% confidence level, while the correlation of MME predictions of IM_SI is as low as 0.37, which is significant only at the 90% level. We have examined predictions of WSI1 850- and 200-hPa components separately and found that the main contribution to the skillful predictions of WSI1 comes from the upper-troposphere component, with the correlation between the observations and MME predictions being 0.63. The correlation between the observed and MME-predicted lower-troposphere component is 0.44

TABLE 3. Temporal correlation coefficients between the observed and model-predicted summer monsoon indices. The single and double asterisks denote the correlation coefficients significant at the 95% and 99% confidence levels, respectively.

	South Asian summer monsoon				Western North Pacific summer monsoon				Northeast Asian summer monsoon			
	WYI	WSI1	IMI	IM_SI	IM_NI	WSI2	WNPMI	WNPM_SI	WNPM_NI	NEASMI	NEASM_SI	NEASM_NI
MME	0.54***	0.63***	0.13	0.37	-0.04	0.66**	0.76**	0.74**	0.63**	0.57**	0.60***	0.21
APCC	0.27	0.40*	0.05	0.18	0	0.42*	0.52**	0.47*	0.48*	0.37	0.42*	0.06
BoM	0.44*	0.56***	0.19	0.44*	0.03	0.68**	0.73**	0.74**	0.62**	0.52**	0.60***	0.32
MSC_CANCM3	0.42*	0.51***	0.01	0.19	-0.1	0.56**	0.54***	0.55***	0.25	0.37	0.45*	-0.06
MSC_CANCM4	0.54***	0.63***	0.02	0.15	-0.15	0.64**	0.71**	0.68**	0.50**	0.31	0.36	0.14
NASA	0.51*	0.59***	0.27	0.35	0.1	0.64**	0.78**	0.76**	0.53**	0.44*	0.62**	0.17
NCEP	0.65***	0.68***	0.14	0.36	-0.05	0.55**	0.57**	0.62**	0.32	0.53**	0.57***	0.08
PNU	0.43*	0.49*	0.09	0.32	0.02	0.55**	0.63**	0.57**	0.65**	0.56**	0.54***	0.16

(significant at the 95% confidence level), which is higher but comparable with that of IM_SI. Gridpoint correlations (Fig. 5) also show that the U200 anomalies over the WSI1 domain are predicted much skillfully than those of U850.

WSI2 and WNPMI represent the variability of WNPSM (B. Wang et al. 2001). The indices indicate the vertical and horizontal circulations associated with WNPSM, respectively (Wang and Fan 1999; B. Wang et al. 2001). These two indices are highly correlated with each other with a correlation coefficient of 0.92. Both WSI2 and WNPMI are well predicted by the models, with TCCs of 0.66 and 0.76 for the MME, respectively, which exceeds the 99% confidence level, and the prediction skill of WNPMI is higher than that of WSI2 (Table 3). For most of the individual models, WSI2 and WNPMI also show high TCCs with the observations exceeding the 99% confidence level, and the TCCs for WNPMI are higher than those for WSI2. This indicates that horizontal circulation in the lower troposphere is simulated better than vertical circulation over the western North Pacific in most of the models. Also, the predictive skill of WNPMI simulated by all models except for NCEP is higher than that of indices related to SASM and the northeastern Asian summer monsoon (NEASM).

The prediction skill of the two components of WNPMI is also assessed separately. Both WNPM_SI and WNPM_NI are skillfully simulated by the MME with TCCs of 0.74 and 0.63, respectively (Table 3). For most of the individual models, the TCC for WNPM_SI is higher than that for WNPM_NI and exceeds the 99% confidence level. However, two models, those of Pusan National University (PNU) and APCC, predict WNPM_NI more skillfully than WNPM_SI does. For the sample size of 28 predictions, the difference between the TCCs obtained for WNPM_NI and WNPM_SI by the MME and by each individual model is insignificant at the 95% confidence level. Therefore, the difference should be treated as occasional, and our comparison results are more qualitative than quantitative, although the difference concurs with results from the previous studies on the seasonal predictability using AGCM and CGCM, which pointed to higher prediction skill in the tropics as compared with the subtropics (Peng et al. 2000; Kumar et al. 2007; Lee and Wang 2012; Kim et al. 2016). In general, it could be concluded that WNPMI and both of its components are well predicted, with TCCs exceeding the 99% confidence level for the MME and for most of the individual models.

While SASM and WNPSM are tropical phenomena, NEASM is a combination of tropical and extratropical monsoons (Ding and Chan 2005). Variations of NEASMI

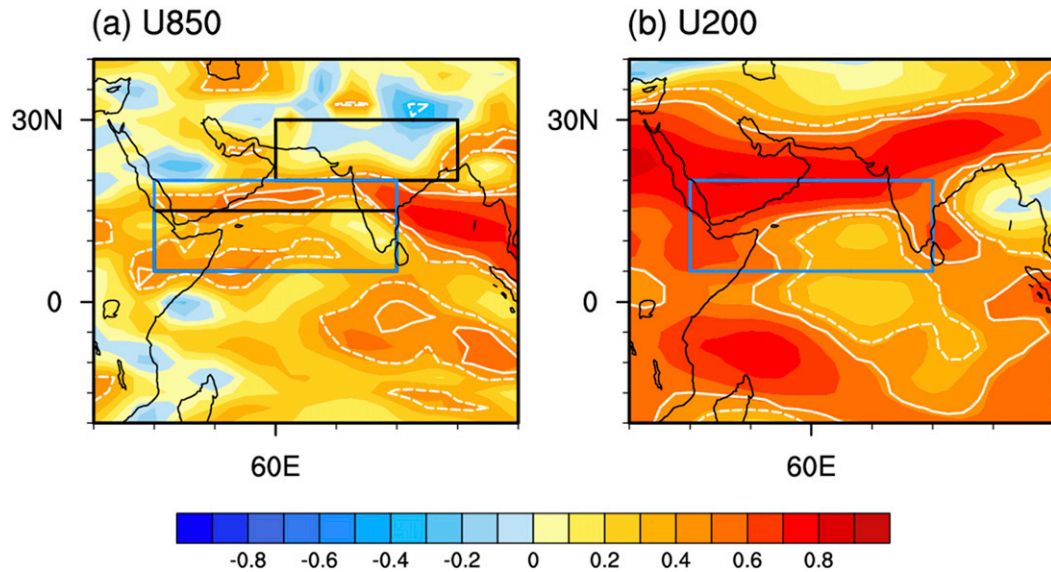


FIG. 5. Correlation coefficients of (a) U850 and (b) U200 between the observations and the MME. The white solid (dashed) line denotes the correlation coefficients significant at the 99% (95%) confidence level. The black boxes denote the domains of IMI and the blue boxes denote the domain of WSI1.

are skillfully simulated by the MME with TCC of 0.57, which exceeds the 99% confidence level (Table 3). Most of the individual models simulate NEASMI with TCCs exceeding the 95% confidence level. Meanwhile, the main contribution to the NEASMI prediction skill comes from the successful predictions of NEASM_SI, with insignificant TCCs between the predicted and observed NEASM_NI. That is, the MME and individual models are able to predict subtropical NEASM_SI zonal wind anomalies but fail to predict the midlatitude zonal wind anomalies associated with NEASM_NI, which corresponds to spatial peculiarities of predictability by dynamic models as revealed in previous studies (e.g., Lee et al. 2005). Nonetheless, even with contribution from only NEASM_SI, the predictions of NEASMI are skillful.

4. Discussion on the sources of predictability

The results from the predictability assessments demonstrate the capability of the APCC MME to predict reliably the zonal-wind-based Asian monsoon indices. In this section, we analyze and discuss the sources of this prediction skill.

The main source of seasonal predictability is slowly varying boundary conditions, particularly tropical SST, which govern the seasonal integrations by the CGCMs (Charney and Shukla 1981; Reichler and Roads 2003; Zhu and Shukla 2013; Vigaud et al. 2017).

Two major convective heat sources that drive the Asian summer monsoons are the convection over

the Bay of Bengal–India–Arabian Sea and that over the South China and Philippine Seas (Y. Wang et al. 2001). Also, the Asian summer monsoons are controlled by slowly varying tropical SST (Yang and Lau 1998; Chang et al. 2000; Wang et al. 2008; Fan et al. 2016). To compare the boundary conditions defining the seasonal-mean status of the Asian summer monsoons, we analyze the observed and simulated SST–monsoon relationships. The concurrent correlation maps between SST anomalies and the indices of SASM, WNPSM, and NEASM observed and predicted by the MME are shown in Figs. 6–8, respectively. The purple lines in the figures denote the threshold values of the correlation coefficient with the 95% confidence level.

Figure 6 shows the correlation maps between SST anomalies and the SASM indices of the observations and MME predictions, respectively. For SASM, in the observations, WYI and WSI1 have statistically significant negative correlations with the SST anomalies over the western and northern Indian Ocean and the tropical eastern Pacific Ocean (Figs. 6a,c). The pattern is similar to that of the negative phase of the Indian Ocean Basin (IOB) index (Yang et al. 2007). The correlation patterns between the SASM indices and the SST anomalies for the MME resemble the observations, but the relationships between them are stronger than in the observations (Figs. 6b,d). Also, in contrast to the observations, the La Niña-like pattern is exposed in the Pacific Ocean in the MME.

IMI and its northern component, IM_NI, in the observations are insignificantly correlated with overall

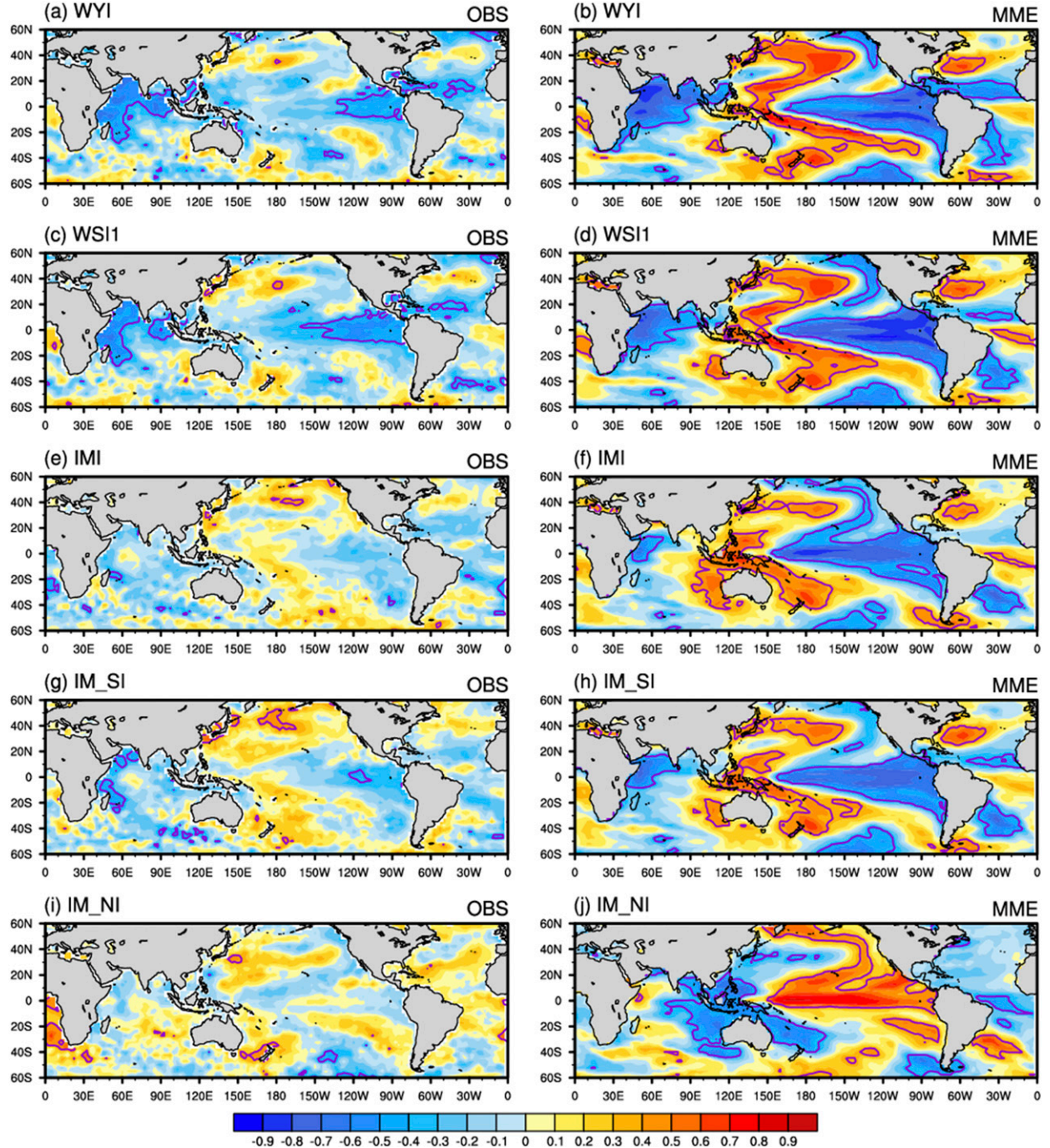


FIG. 6. Correlation maps between the SST anomalies and SASM indices from the (a),(c),(e),(g),(i) observations and (b),(d),(f),(h),(j) MME predictions during 1983–2010. The contours denote the correlation coefficients significant at the 95% confidence level.

SST, which implies that its seasonal predictability cannot be attributed to the summer SST boundary conditions (Figs. 6e,i). Only the southern component, IM_SI, significantly negatively correlates with Arabian Sea SST (Fig. 6g). However the relationships of IMI and both its components with SST in the MME are strong, and the

correlation patterns are similar to those of WYI and WSI1 in the MME (Figs. 6f,h,j).

Unlike SASM, WSI2 and WNPMI, representing WNPSM, significantly negatively correlate with the SST anomalies over the Arabian Sea–Bay of Bengal–Philippine Sea, and positively correlate with the SST

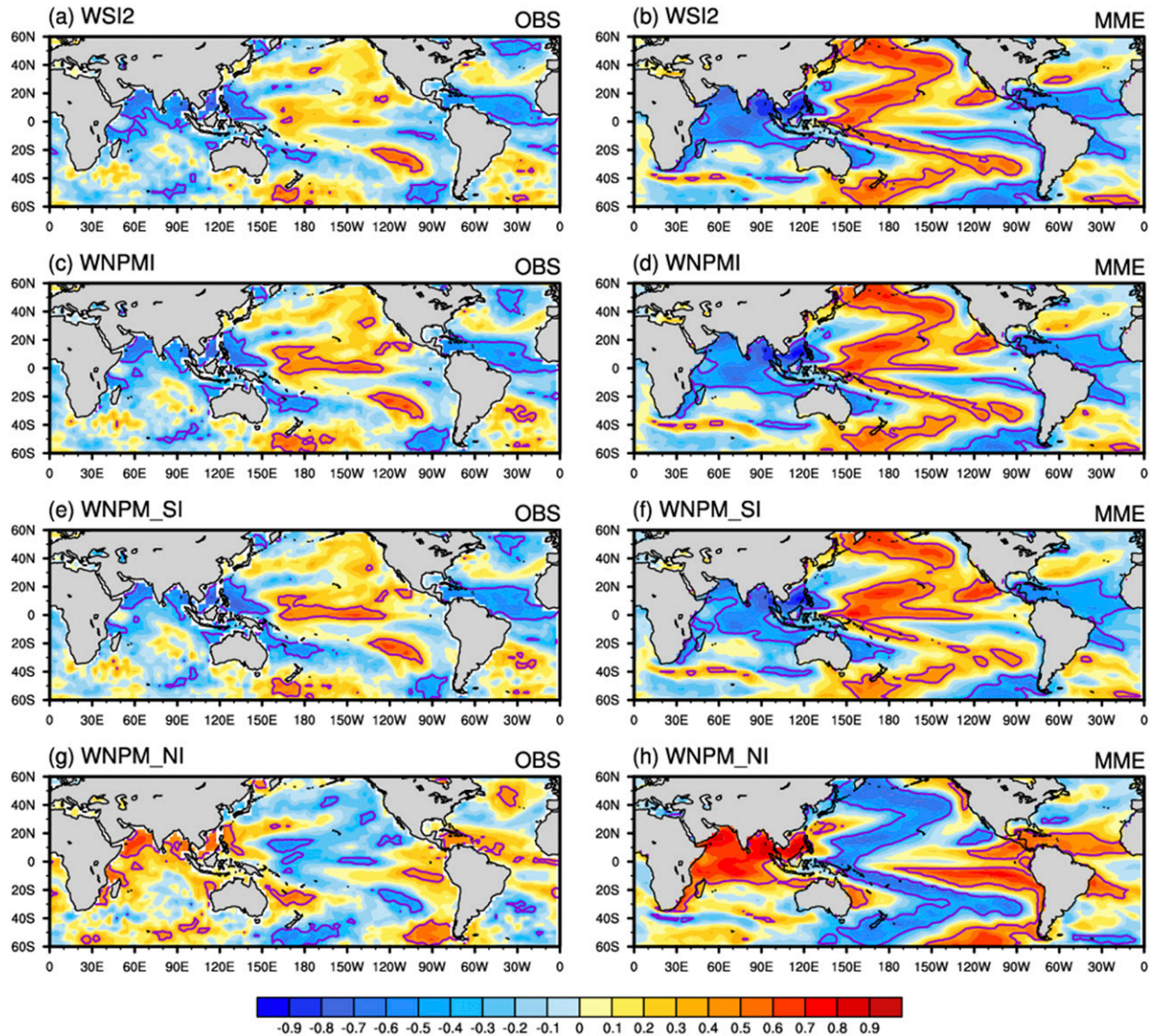


FIG. 7. Correlation maps between the SST anomalies and WNPMI indices and the WNPMI components from the (a),(c),(e),(g) observations and (b),(d),(f),(h) MME predictions during 1983–2010. The contours denote the correlation coefficients significant at the 95% confidence level.

anomalies over the central tropical Pacific (Yeh et al. 2009) (Figs. 7a,c). WSI2 and WNPMI seem to be more related to the El Niño Modoki (Ashok et al. 2007) than to classical ENSO. The correlation patterns between SST anomalies and the WNPMI indices in the MME are more significant in the wider area than in the observations and the correlations are stronger (Figs. 7b and 6d).

NEASMI in the observations is significantly positively correlated with SST anomalies over the north Indian Ocean–South China Sea and the eastern tropical Pacific, and negatively with the SST anomalies near East Asia (Fig. 8a). The correlation pattern for the MME is similar to that of the observations, but the relationships between

SST and NEASMI are stronger in the MME than those in the observations (Fig. 8b). The correlation maps between the SST anomalies and the components of NEASMI based on the observations are shown in Figs. 8c and 8e. NEASMI_SI, the southern component of NEASMI, strongly correlates with the SST anomalies over the north Indian Ocean and slightly weakly with those over the eastern tropical Pacific (Fig. 8c), with the MME-based correlation pattern resembling it (Fig. 8d). NEASMI_NI, the northern component of NEASMI, strongly correlates with the SST anomalies over the easternmost tropical Pacific (Fig. 8e). However, the MME-based pattern closely resembles that of classical El Niño (Fig. 8f).

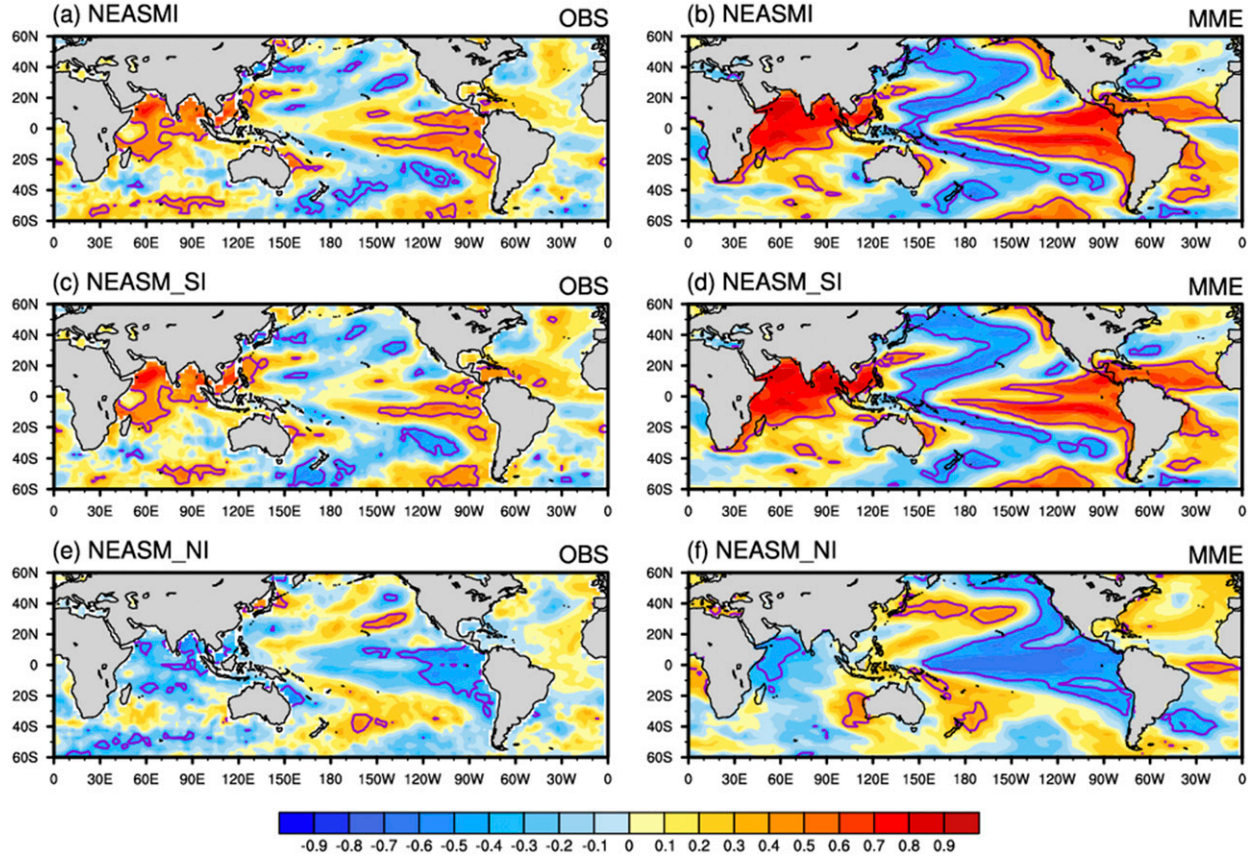


FIG. 8. Correlation maps between the SST anomalies and the NEASMI index and its components from the (a),(c),(e) observations and (b),(d),(f) MME predictions during 1983–2010. The contours denote the correlation coefficients significant at the 95% confidence level.

All the analyzed summer monsoon indices, with the exception of IMI, are highly correlated with the SST anomalies over the global ocean, particularly in the tropics. The correlation coefficients between the summer monsoon indices and the tropical SST indices for both the observations and MME were calculated to compare the relationships of the interannual variability between them (Fig. 9). The tropical SST indices used in this study are Niño-1+2 (10°S – 0° , 90° – 80°W ; Trenberth and Stepaniak 2001), Niño-3.4 (5°S – 5°N , 170° – 120°W ; Trenberth and Stepaniak 2001), IOB (20°S – 20°N , 40° – 110°E ; Yang et al. 2007) and Indian Ocean dipole (IOD; 10°S – 10°N , 50° – 70°E minus 10°S – 0° , 90° – 110°E ; Saji et al. 1999).

In the observations, WYI significantly correlates only with IOB (99% level) and Niño-1+2 (95% level) indices. Meanwhile, the MME significantly correlates with all four SST indices (Fig. 9a), indicating that its predictability is based on the successful simulation of the significant relationships of WYI with IOB by the MME (correlations are -0.63 in the observations and -0.67 in the MME). However, in the model

simulations WYI significantly correlates (above 99% confidence level) with the ENSO-related indices and with IOD, which deteriorates the prediction skill because there are no such significant relationships in the observations. The correlation between WSI1 and IOB is significantly negative in both the MME and observations with similar values, but the relationships with other SST indices in the MME are simulated larger compared with the observations (Fig. 9b). The poorly predictable IMI and both its components do not feature any significant correlations with SST indices in the observations. However, in the MME, all three significantly (at least at the 95% confidence level) correlate with the ENSO-related indices and IOD (Figs. 9c,d,e).

Three WNPSM indices (WSI2, WNPMI, and WNPM_SI) are significantly negatively correlated with IOB in both the MME and the observations, although the values in the MME are slightly higher than in the observations (Figs. 9f–i). Also, WNPM_SI is significantly positively correlated with Niño-3.4 in the observations, and the MME simulates these relationships successfully.

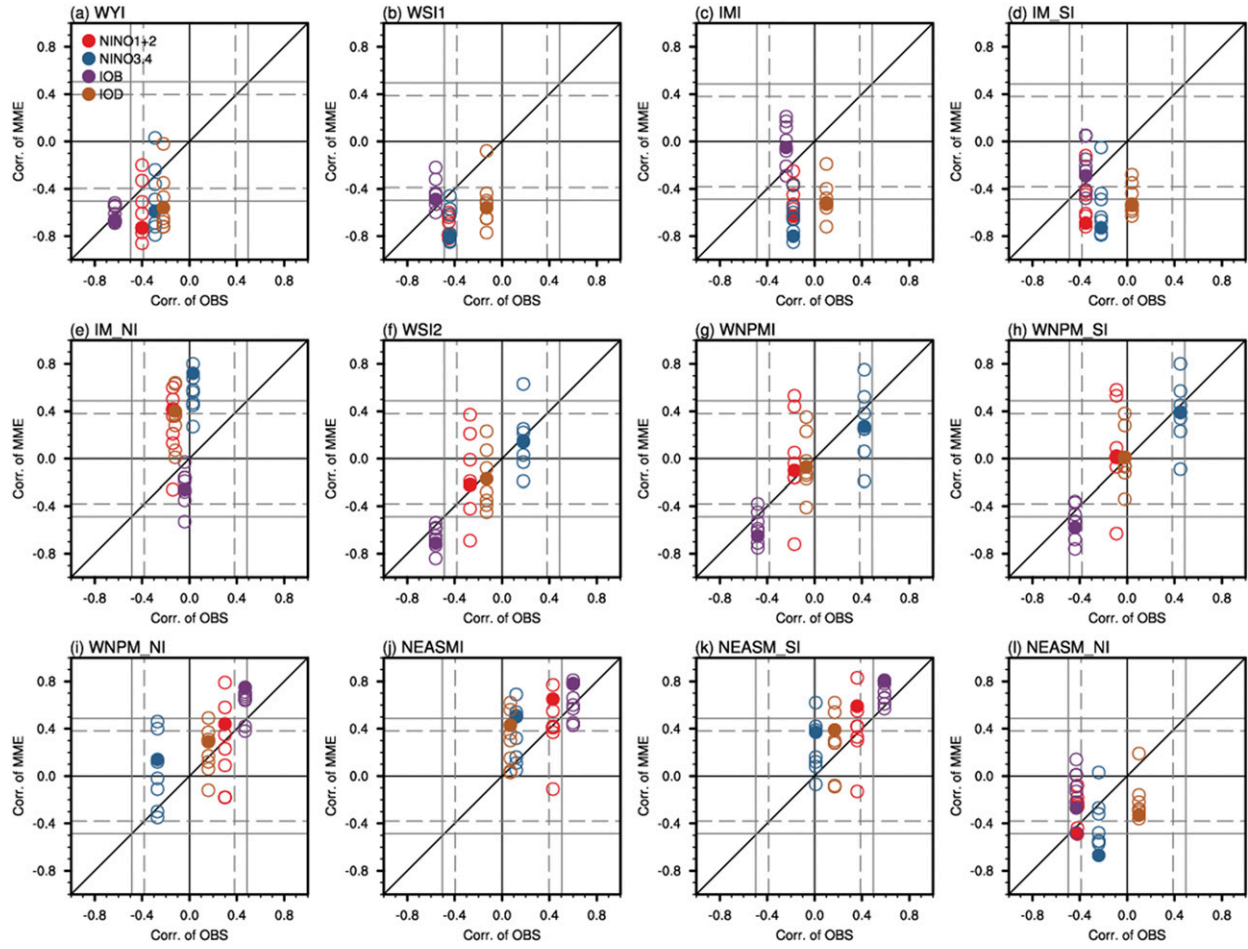


FIG. 9. Correlation coefficients between the tropical SST indices (Niño-1+2, Niño-3.4, IOB, and IOD) and summer monsoon indices derived from the observations and the MME predictions. The summer monsoon index is indicated in the top-left corner of each panel. The correlation coefficients between the SST indices and the MME (individual model) predictions are shown with closed (open) circles. The SST indices are indicated with the colors shown in (a). The solid (dashed) gray lines denote the 99% (95%) confidence level.

WNPM_NI significantly positively correlates with IOB in the observations but not with any other indices in either the observations or MME except with Niño-1+2 in MME.

In the observations, NEASMI and NEASM_SI are related to IOB, with correlations exceeding the 99% confidence level, and the correlation between NEASMI and the Niño-1+2 index exceeds the 95% confidence level (Figs. 9j,k). Similarly in the MME, both NEASMI and NEASM_SI significantly correlate with both IOB and Niño-1+2, with correlation coefficients exceeding those obtained in the observations. NEASM_NI in the observations significantly correlates with IOB and Niño-1+2 (the 95% confidence level). However, in the MME it has the strongest correlation with Niño-3.4 (-0.67). Also, the NEASM_NI relationships with the tropical SST anomalies and indices are the weakest among all the monsoon indices.

Indeed, the associated NEASM_NI midlatitude circulation anomalies are strongly affected by the processes in the middle and high latitudes (e.g., Ding and Chan 2005; Lee et al. 2005), which weakens the influence from the tropics.

With exception of NEASM_NI and IMI, all the monsoon indices in both the observations and MME are strongly related to IOB, with the correlations exceeding the 95% confidence level. The differences between these correlations obtained in the observations and the MME are insignificant at the 95% confidence level and can be considered occasional (Fig. S1 in the online supplemental material). This explains the high prediction skill of these indices by the MME. Particularly, the WNPSM indices, WSI2 and WNPMI and its components, with correlations between the observations and MME ranging within 0.63–0.76, in both the observations and MME, are strongly related to the

same SST indices. Two SASM indices, WYI and WSI1, in both the observations and MME predictions are strongly related to IOB. However, although it is the only significant relationship in the observations, in the MME they also correlate with the Niño indices, with correlations exceeding 0.59. This partially explains the decrease of the correlations between the observed and MME-predicted SASM indices down to 0.54–0.63; nonetheless, they remain significant at the 99% confidence level. NEASMI and its southern component, NEASM_SI, are well predicted by the MME with correlations of 0.57 and 0.60, respectively, because, similarly to the WNPSM indices, in both the observations and MME they are related to the same SST patterns and indices. The prediction skill of NEASM_NI is low because the models do not capture its relationships with Niño-1+2; instead, they strongly relate it to Niño-3.4.

In general, the SST correlation patterns and the correlations with the SST indices obtained on the MME predictions are largely consistent with those obtained in the observations for all the analyzed monsoon indices and their components, with the exception of NEASM_NI and IMI. Although the observation-based patterns are much noisier than those obtained for the MME predictions, and despite the correlations with the observation-based SST indices being slightly lower than those obtained on the MME predictions, this consistency explains the high prediction skill of all the analyzed monsoon indices and their components, with the exception of NEASM_NI and IMI.

The correlation patterns of the SST anomalies in the MME predictions are more pronounced and stronger than those in the observations for all the analyzed monsoon indices. On one hand, this may be due to exclusion of the stochastic weather noise in the model simulations that are deterministic in their nature; on the other hand, it may reflect the loss of some climate links not described in the models because of their simplification as compared with the original climate system. Similarly, the relationships between the monsoon indices and the SST indices are stronger in the MME than in the observations. This is consistent with the results of Kim et al. (2012), who have shown overestimation of the relationships between SASM and ENSO using two CGCMs, and of Li et al. (2012) and (2014), who documented overestimation of the relationships between WNPSM and ENSO in model simulations.

Most of the summer monsoon indices are well correlated with the summer IOB in both the MME predictions and observations. Previous studies (Cherchi et al. 2007; Yang et al. 2007; Li et al. 2008; Kosaka

et al. 2013) have also shown the impact of the summer IOB on the Asian summer monsoons. According to Yang et al. (2007) and Li et al. (2008), the Indian Ocean warming forces a Gill-type response in the upper troposphere with the intensified South Asian high, so that the southwest monsoon intensifies over the Arabian Sea and weakens over the South China and Philippine Seas. In addition, an anomalous anticyclonic circulation forms over the subtropical northwestern Pacific, enhancing the western North Pacific subtropical high, which in turn enhances NEASM (Lee et al. 2006; S.-S. Lee et al. 2013). The summer IOB mode is a favored mode of the growing and decaying phases of ENSO, but it can also occur without ENSO (Kug et al. 2006; Kosaka et al. 2013). Previous studies have also shown that the effect of ENSO on the Asian summer monsoons appears through the teleconnection with the time lag (Kawamura 1998; Wang and Zhang 2002). This time lag could be a cause of the stronger concurrent relationships of the Asian summer monsoons with the summer IOB than with ENSO.

5. Summary

In this study, the seasonal prediction skill of Asian summer monsoon indices based on the zonal wind was investigated using the 1-month-lead hindcast datasets from seven CGCMs participating in the operational MME seasonal prediction system of APCC for the boreal summers of 1983–2010. The summer monsoon indices investigated in this study present the variations of SASM, WNPSM, and NEASM.

The prediction skill from the models demonstrates the superior capability of the MME to reproduce the variations of most of the monsoon indices characterizing SASM, WNPSM, and NEASM. Two SASM indices, WYI and WSI1, are well predicted by the MME with correlations of 0.54–0.63 exceeding the 99% confidence level. The correlation coefficients of the WNPSM indices between the observations and the MME are the highest at 0.66–0.76. The interannual variations of WNPMI are well reproduced in all the individual models with a 99% confidence level, and both the components of WNPMI are well simulated in the MME and in most of the individual models. The MME and the individual models have a poor capability to simulate NEASM_NI because they relate it mainly to the forcing from the central equatorial Pacific (Niño-3.4), whereas in the observations it is mainly related to the easternmost Pacific forcing (Niño-1+2) because NEASM_NI is affected not only by the variability in the tropics but also by the climate variability in the middle and high latitudes.

With the exception of NEASM_NI, IMI, and IM_NI, all the monsoon indices in both the observations and MME are strongly related to the SST anomalies in the north Indian Ocean, with the difference between the correlations obtained from the observations and MME predictions being insignificant. For SASM indices (WSI1 and WYI), the MME is skillful in reproducing their relationships with the north Indian Ocean SST anomalies; however, in the MME predictions, these indices also have strong relationships with the ENSO-related SST anomalies, while there are no such significant relationships in the observations. For WNPSM, the MME skillfully captures the correlations with the SST anomalies over the Indian and Pacific Oceans and simulates the relationships between the WNPSM indices (WSI2 and WNPMI) and SST indices (IOB and Niño-3.4), similar to those in the observations. For NEASM and its southern component (NEASM_SI), the MME successfully captures its relationships with the SST anomalies over the Indian Ocean and the tropical easternmost Pacific, but the power is slightly stronger than in the observations.

Using 1-month-lead hindcast outputs of the seven CGCMs of the APCC seasonal prediction system, we have demonstrated that the APCC MME predictions are capable of reliably predicting most of the Asian summer monsoons in terms of the monsoon indices based on the zonal wind anomalies. The Asian summer monsoons are mostly affected by the slowly varying SST anomalies, both concurrently and with various time lags. Thus, future research should analyze the CGCMs' predictions with lead times longer than one month in order to assess whether the effects of preceding SST variability on the summer monsoons are well simulated in the CGCMs.

Our study has revealed that skillful simulation of the Asian summer monsoon will require further improvement of the CGCMs by focusing on enhancing the prediction of the Indian Ocean SST anomalies and their impact on the evolution of monsoon circulation, which is suppressed by the ENSO-originated forcing in the current state-of-the-art CGCMs.

Acknowledgments. The authors appreciate the APEC Climate Center and participating institutes of the APCC operational MME seasonal prediction system for providing hindcast data. This work was carried out with support of the Rural Development Administration Cooperative Research Program for Agriculture Science and Technology Development under Grant Project PJ01229302 and the Korea Meteorological Administration Research and Development Program under Grant KMI2018-01213.

REFERENCES

- Adler, R. F., and Coauthors, 2003: The Version-2 Global Precipitation Climatology Project (GPCP) monthly precipitation analysis (1979–present). *J. Hydrometeor.*, **4**, 1147–1167, [https://doi.org/10.1175/1525-7541\(2003\)004<1147:TVGPCP>2.0.CO;2](https://doi.org/10.1175/1525-7541(2003)004<1147:TVGPCP>2.0.CO;2).
- Ashok, K., S. K. Behera, S. A. Rao, H. Weng, and T. Yamagata, 2007: El Niño Modoki and its possible teleconnection. *J. Geophys. Res.*, **112**, C11007, <https://doi.org/10.1029/2006JC003798>.
- Bretherton, C. S., M. Widmann, V. P. Dymnikov, J. M. Wallace, and I. Bladé, 1999: The effective number of spatial degrees of freedom of a time-varying field. *J. Climate*, **12**, 1990–2009, [https://doi.org/10.1175/1520-0442\(1999\)012<1990:TENOSD>2.0.CO;2](https://doi.org/10.1175/1520-0442(1999)012<1990:TENOSD>2.0.CO;2).
- Chang, C.-P., Y. Zhang, and T. Li, 2000: Interannual and interdecadal variations of the East Asian summer monsoon and tropical Pacific SSTs. Part I: Roles of the subtropical ridge. *J. Climate*, **13**, 4310–4325, [https://doi.org/10.1175/1520-0442\(2000\)013<4310:IAIVOT>2.0.CO;2](https://doi.org/10.1175/1520-0442(2000)013<4310:IAIVOT>2.0.CO;2).
- Charney, J. G., and J. Shukla, 1981: Predictability of monsoons. *Monsoon Dynamics*, J. Lighthill and R. P. Pearce, Eds., Cambridge University Press, 99–109.
- Cherchi, A., S. Gualdi, S. Behera, J. J. Luo, S. Masson, T. Yamagata, and A. Navarra, 2007: The influence of tropical Indian Ocean SST on the Indian summer monsoon. *J. Climate*, **20**, 3083–3105, <https://doi.org/10.1175/JCLI4161.1>.
- Day, J. A., I. Fung, and C. Risi, 2015: Coupling of South and East Asian monsoon precipitation in July–August. *J. Climate*, **28**, 4330–4356, <https://doi.org/10.1175/JCLI-D-14-00393.1>.
- Ding, Y. H., 2004: Seasonal march of the East Asian summer monsoon. *East Asian Monsoon*, C.-P. Chang, Ed., World Scientific Series on Meteorology of East Asia, Vol. 2, World Scientific Publisher, 3–53.
- , and J. C. L. Chan, 2005: The East Asian summer monsoon: An overview. *Meteor. Atmos. Phys.*, **89**, 117–142, <https://doi.org/10.1007/s00703-005-0125-z>.
- Fan, L., S.-I. Shin, Z. Liu, and Q. Liu, 2016: Sensitivity of Asian summer monsoon precipitation to tropical sea surface temperature anomalies. *Climate Dyn.*, **47**, 2501–2514, <https://doi.org/10.1007/s00382-016-2978-x>.
- Goswami, B. N., B. Krishnamurthy, and H. Annamalai, 1999: A broad-scale circulation index for interannual variability of the Indian summer monsoon. *Quart. J. Roy. Meteor. Soc.*, **125**, 611–633, <https://doi.org/10.1002/qj.49712555412>.
- Ha, K. J., S. K. Park, and K. Y. Kim, 2005: On interannual characteristics of Climate Prediction Center merged analysis precipitation over the Korean Peninsula during the summer monsoon season. *Int. J. Climatol.*, **25**, 99–116, <https://doi.org/10.1002/joc.1116>.
- Hamill, T. M., 2001: Interpretation of rank histograms for verifying ensemble forecasts. *Mon. Wea. Rev.*, **129**, 550–560, [https://doi.org/10.1175/1520-0493\(2001\)129<0550:IORHFV>2.0.CO;2](https://doi.org/10.1175/1520-0493(2001)129<0550:IORHFV>2.0.CO;2).
- Jung, M.-I., S.-W. Son, J. Choi, and H.-S. Kang, 2015: Assessment of 6-month lead prediction skill of the GloSea5 hindcast experiment (in Korean). *Atmosphere*, **25**, 1–15.
- Kanamitsu, M., W. Ebisuzaki, J. Woollen, S.-K. Yang, J. J. Hnilo, M. Fiorino, and G. L. Potter, 2002: NCEP–DOE AMIP-II Reanalysis (R-2). *Bull. Amer. Meteor. Soc.*, **83**, 1631–1643, <https://doi.org/10.1175/BAMS-83-11-1631>.
- Kang, I.-S., and Coauthors, 2002: Intercomparison of the climatological variations of Asian summer monsoon precipitation simulated by 10 GCMs. *Climate Dyn.*, **19**, 383–395, <https://doi.org/10.1007/s00382-002-0245-9>.

- Kawamura, R., 1998: A possible mechanism of the Asian summer monsoon-ENSO coupling. *J. Meteor. Soc. Japan*, **76**, 1009–1027, https://doi.org/10.2151/jmsj1965.76.6_1009.
- Kim, G., and Coauthors, 2016: Global and regional skill of the seasonal predictions by WMO Lead Centre for Long-Range Forecast Multi-Model Ensemble. *Int. J. Climatol.*, **36**, 1657–1675, <https://doi.org/10.1002/joc.4449>.
- Kim, H.-M., P. J. Webster, J. A. Curry, and V. E. Toma, 2012: Asian summer monsoon prediction in ECMWF System 4 and NCEP CFSv2 retrospective seasonal forecasts. *Climate Dyn.*, **39**, 2975–2991, <https://doi.org/10.1007/s00382-012-1470-5>.
- Kosaka, Y., and H. Nakamura, 2006: Structure and dynamics of the summertime Pacific–Japan teleconnection pattern. *Quart. J. Roy. Meteor. Soc.*, **132**, 2009–2030, <https://doi.org/10.1256/qj.05.204>.
- , S.-P. Xie, N.-C. Lau, and G. A. Vecchi, 2013: Origin of seasonal predictability for summer climate over the northwestern Pacific. *Proc. Natl. Acad. Sci. USA*, **110**, 7574–7579, <https://doi.org/10.1073/pnas.1215582110>.
- Kubota, H., Y. Kosaka, and S.-P. Xie, 2016: A 117-year long index of the Pacific–Japan pattern with application to interdecadal variability. *Int. J. Climatol.*, **36**, 1575–1589, <https://doi.org/10.1002/joc.4441>.
- Kug, J.-S., T. Li, S.-I. An, I.-S. Kang, J.-J. Luo, S. Masson, and T. Yamagata, 2006: Role of the ENSO–Indian Ocean coupling on ENSO variability in a coupled GCM. *Geophys. Res. Lett.*, **33**, L09710, <https://doi.org/10.1029/2005GL024916>.
- Kumar, A., B. Jha, Q. Zhang, and L. Bounoua, 2007: A new methodology for estimating the unpredictable component of seasonal atmospheric variability. *J. Climate*, **20**, 3888–3901, <https://doi.org/10.1175/JCLI4216.1>.
- Lau, K.-M., M.-K. Kim, and S. Yang, 2000: Dynamical and boundary forcing characteristics of regional components of the Asian summer monsoon. *J. Climate*, **13**, 2461–2482, [https://doi.org/10.1175/1520-0442\(2000\)013<2461:DABFCO>2.0.CO;2](https://doi.org/10.1175/1520-0442(2000)013<2461:DABFCO>2.0.CO;2).
- Lee, D. Y., J.-B. Ahn, and K. Ashok, 2013: Improvement of multimodel ensemble seasonal prediction skills over East Asian summer monsoon region using a climate filter concept. *J. Appl. Meteor. Climatol.*, **52**, 1127–1138, <https://doi.org/10.1175/JAMC-D-12-0123.1>.
- Lee, E.-J., J.-G. Jhun, and C.-K. Park, 2005: Remote connection of the northeast Asian summer rainfall variation revealed by a newly defined monsoon index. *J. Climate*, **18**, 4381–4393, <https://doi.org/10.1175/JCLI3545.1>.
- , S.-W. Yeh, J.-G. Jhun, and B.-K. Moon, 2006: Seasonal change in anomalous WNPSH associated with the strong East Asian summer monsoon. *Geophys. Res. Lett.*, **33**, L21702, <https://doi.org/10.1029/2006GL027474>.
- Lee, J.-Y., and B. Wang, 2012: Seasonal climate prediction and predictability of atmospheric circulation. *Climate Models*, L. M. Druyan, Ed., IntechOpen, 19–42, <https://doi.org/10.5772/33782>.
- Lee, S.-S., Y.-W. Seo, K.-J. Ha, and J.-G. Jhun, 2013: Impact of the western North Pacific subtropical high on the East Asian monsoon precipitation and the Indian Ocean precipitation in the boreal summertime. *Asia-Pac. J. Atmos. Sci.*, **49**, 171–182, <https://doi.org/10.1007/s13143-013-0018-x>.
- Li, C., R. Lu, and B. Dong, 2012: Predictability of the western North Pacific summer climate demonstrated by the coupled models of ENSEMBLES. *Climate Dyn.*, **39**, 329–346, <https://doi.org/10.1007/s00382-011-1274-z>.
- , —, and —, 2014: Predictability of the western North Pacific summer climate associated with different ENSO phases by ENSEMBLES multi-model seasonal forecasts. *Climate Dyn.*, **43**, 1829–1845, <https://doi.org/10.1007/s00382-013-2010-7>.
- Li, J., and Q. Zeng, 2002: A unified monsoon index. *Geophys. Res. Lett.*, **29**, 1274, <https://doi.org/10.1029/2001GL013874>.
- Li, S., J. Lu, G. Huang, and K. Hu, 2008: Tropical Indian Ocean basin warming and East Asian summer monsoon: A multiple AGCM study. *J. Climate*, **21**, 6080–6088, <https://doi.org/10.1175/2008JCLI2433.1>.
- Lu, R.-Y., C.-F. Li, S. H. Yang, and B. Dong, 2012: The coupled model predictability of the western North Pacific summer monsoon with different leading times. *Atmos. Ocean. Sci. Lett.*, **5**, 219–224, <https://doi.org/10.1080/16742834.2012.11447000>.
- Min, Y.-M., V. N. Krylov, and S. M. Oh, 2014: Assessment of APCC multimodel ensemble prediction in seasonal climate forecasting: Retrospective (1983–2003) and real-time forecasts (2008–2013). *J. Geophys. Res. Atmos.*, **119**, 12 132–12 150, <https://doi.org/10.1002/2014JD022230>.
- , —, —, and H.-J. Lee, 2017: Skill of real-time operational forecasts with the APCC multi-model ensemble prediction system during the period 2008–2015. *Climate Dyn.*, **49**, 4141–4156, <https://doi.org/10.1007/s00382-017-3576-2>.
- Peng, P., A. Kumar, A. G. Barnston, and L. Goddard, 2000: Simulation skills of the SST-forced global climate variability of the NCEP-MRF9 and the Scripps–MPI ECHAM3 models. *J. Climate*, **13**, 3657–3679, [https://doi.org/10.1175/1520-0442\(2000\)013<3657:SSOTSF>2.0.CO;2](https://doi.org/10.1175/1520-0442(2000)013<3657:SSOTSF>2.0.CO;2).
- Reichler, T. J., and J. O. Roads, 2003: The role of boundary and initial conditions for dynamical seasonal predictability. *Nonlinear Processes Geophys.*, **10**, 211–232, <https://doi.org/10.5194/npg-10-211-2003>.
- Reynolds, R. W., N. A. Rayner, T. M. Smith, D. C. Stokes, and W. Wang, 2002: An improved in situ and satellite SST analysis. *J. Climate*, **15**, 1609–1625, [https://doi.org/10.1175/1520-0442\(2002\)015<1609:AIISAS>2.0.CO;2](https://doi.org/10.1175/1520-0442(2002)015<1609:AIISAS>2.0.CO;2).
- Saji, N. H., B. N. Goswami, P. N. Vinayachandran, and T. Yamagata, 1999: A dipole mode in the tropical Indian Ocean. *Nature*, **401**, 360–363, <https://doi.org/10.1038/43854>.
- Shi, N., and Q. G. Zhu, 1996: An abrupt change in the intensity of the East Asian summer monsoon index and its relationship with temperature and precipitation over east China. *Int. J. Climatol.*, **16**, 757–764, [https://doi.org/10.1002/\(SICI\)1097-0088\(199607\)16:7<757::AID-JOC50>3.0.CO;2-5](https://doi.org/10.1002/(SICI)1097-0088(199607)16:7<757::AID-JOC50>3.0.CO;2-5).
- Sohn, S.-J., Y.-M. Min, J.-Y. Lee, C.-Y. Tam, I.-S. Kang, B. Wang, J.-B. Ahn, and T. Yamagata, 2012: Assessment of the long-lead probabilistic prediction for the Asian summer monsoon precipitation (1983–2011) based on the APCC multimodel system and a statistical model. *J. Geophys. Res.*, **117**, D04102, <https://doi.org/10.1029/2011JD016308>.
- Trenberth, K. E., and D. P. Stepaniak, 2001: Indices of El Niño evolution. *J. Climate*, **14**, 1697–1701, [https://doi.org/10.1175/1520-0442\(2001\)014<1697:LIOENO>2.0.CO;2](https://doi.org/10.1175/1520-0442(2001)014<1697:LIOENO>2.0.CO;2).
- Vigaud, N., A. W. Robertson, M. K. Tippett, and N. Acharya, 2017: Subseasonal predictability of boreal summer monsoon rainfall from ensemble forecasts. *Front. Environ. Sci.*, **5**, 67, <https://doi.org/10.3389/fenvs.2017.00067>.
- Wang, B., and Z. Fan, 1999: Choice of South Asian summer monsoon indices. *Bull. Amer. Meteor. Soc.*, **80**, 629–638, [https://doi.org/10.1175/1520-0477\(1999\)080<0629:COSASM>2.0.CO;2](https://doi.org/10.1175/1520-0477(1999)080<0629:COSASM>2.0.CO;2).
- , —, and Q. Zhang, 2002: Pacific–East Asian teleconnection. Part II: How the Philippine Sea anomalous anticyclone is established during El Niño development. *J. Climate*, **15**, 3252–3265, [https://doi.org/10.1175/1520-0442\(2002\)015<3252:PEATPI>2.0.CO;2](https://doi.org/10.1175/1520-0442(2002)015<3252:PEATPI>2.0.CO;2).

- , R. Wu, and K.-M. Lau, 2001: Interannual variability of Asian summer monsoon: Contrast between the Indian and the western North Pacific–East Asian monsoons. *J. Climate*, **14**, 4073–4090, [https://doi.org/10.1175/1520-0442\(2001\)014<4073:IVOTAS>2.0.CO;2](https://doi.org/10.1175/1520-0442(2001)014<4073:IVOTAS>2.0.CO;2).
- , Z. Wu, J. Li, J. Liu, C. P. Chang, Y. Ding, and G. Wu, 2008: How to measure the strength of the East Asian summer monsoon. *J. Climate*, **21**, 4449–4463, <https://doi.org/10.1175/2008JCLI2183.1>.
- , and Coauthors, 2009: Advance and prospectus of seasonal prediction: Assessment of the APCC/CLIPAS 14-model ensemble retrospective seasonal prediction (1980–2004). *Climate Dyn.*, **33**, 93–117, <https://doi.org/10.1007/s00382-008-0460-0>.
- Wang, Y., B. Wang, and J.-H. Oh, 2001: Impacts of the preceding El Niño on the East Asian summer atmospheric circulation. *J. Meteor. Soc. Japan*, **79**, 575–588, <https://doi.org/10.2151/jmsj.79.575>.
- Webster, P. J., and S. Yang, 1992: Monsoon and ENSO: Selectively interactive systems. *Quart. J. Roy. Meteor. Soc.*, **118**, 877–926, <https://doi.org/10.1002/qj.49711850705>.
- Wilks, D., 1995: *Statistical Methods in the Atmospheric Sciences: An Introduction*. International Geophysics Series, Vol. 59, Elsevier, 467 pp.
- Yang, J., Q. Liu, S.-P. Xie, Z. Liu, and L. Wu, 2007: Impact of the Indian Ocean SST basin mode on the Asian summer monsoon. *Geophys. Res. Lett.*, **34**, L02708, <https://doi.org/10.1029/2006GL028571>.
- Yang, S., and K.-M. Lau, 1998: Influences of sea surface temperature and ground wetness on Asian summer monsoon. *J. Climate*, **11**, 3230–3246, [https://doi.org/10.1175/1520-0442\(1998\)011<3230:IOSSTA>2.0.CO;2](https://doi.org/10.1175/1520-0442(1998)011<3230:IOSSTA>2.0.CO;2).
- , Z. Zhang, V. E. Kousky, R. W. Higgins, S.-H. Yoo, J. Liang, and Y. Fan, 2008: Simulations and seasonal prediction of the Asian summer monsoon in the NCEP Climate Forecast System. *J. Climate*, **21**, 3755–3775, <https://doi.org/10.1175/2008JCLI1961.1>.
- Yeh, S.-W., J.-S. Kug, B. Dewitte, M.-H. Kwon, B. P. Kritman, and F.-F. Jin, 2009: El Niño in a changing climate. *Nature*, **461**, 511–514, <https://doi.org/10.1038/nature08316>.
- Yuan, X., J. K. Roundy, E. F. Wood, and J. Sheffield, 2015: Seasonal forecasting of global hydrologic extremes: System development and evaluation over GEWEX basins. *Bull. Amer. Meteor. Soc.*, **96**, 1895–1912, <https://doi.org/10.1175/BAMS-D-14-00003.1>.
- Yule, G. U., and M. G. Kendall, 1950: *An Introduction to the Theory of Statistics*. 14th ed. Charles Griffin, 701 p.
- Zhou, T., and Coauthors, 2009a: The CLIVAR C20C Project: Which components of the Asian–Australian monsoon circulation variations are forced and reproducible? *Climate Dyn.*, **33**, 1051–1068, <https://doi.org/10.1007/s00382-008-0501-8>.
- , B. Wu, and B. Wang, 2009b: How well do atmospheric general circulation models reproduce the leading modes of the interannual variability of the Asian–Australian monsoon? *J. Climate*, **22**, 1159–1173, <https://doi.org/10.1175/2008JCLI2245.1>.
- Zhu, J., and J. Shukla, 2013: The role of air-sea coupling in seasonal prediction of Asia-Pacific summer monsoon rainfall. *J. Climate*, **26**, 5689–5697, <https://doi.org/10.1175/JCLI-D-13-00190.1>.